Surface structure and sputtering in amorphous carbon thin films: a tight-binding study of film deposition

2002 J. Phys.: Condens. Matter 14 723

(http://iopscience.iop.org/0953-8984/14/4/307)

INSTITUTE OF PHYSICS PUBLISHING JOURNAL OF PHYSICS: CONDENSED MATTER

J. Phys.: Condens. Matter **14** (2002) 723–730 PII: S0953-8984(02)28660-9

Surface structure and sputtering in amorphous carbon thin films: a tight-binding study of film deposition

N C Cooper, M S Fagan, C M Goringe, N A Marks and D R McKenzie

Department of Applied Physics, School of Physics A28, The University of Sydney, NSW 2006, Australia

E-mail: ncooper@physics.usyd.edu.au

Received 4 September 2001
Published 18 January 2002
Online at stacks.iop.org/JPhysCM/14/723

Abstract

A tight-binding simulation of the atom-by-atom deposition of amorphous carbon (a-C) at 100 eV incident energy is presented. More than 500 atoms were deposited. Chains are observed to form on the surface, some of which are sputtered. The good agreement with the experimental sputter frequency data and observation that all such clusters are linear provides strong support for the existence of these chains and the direct emission model of sputtering. The bulk of the grown film is a-C with a tetrahedral bonding fraction of 20%. Experiments have shown that at this incident energy of 100 eV, tetrahedral a-C is the preferred structural form rather than the a-C produced by this simulation. This discrepancy is attributed to the short range of the interatomic potential.

1. Introduction

Amorphous carbon (a-C) is a material with a wide range of properties, allowing it to be engineered for useful applications such as in hard coatings and electronics. In many of these applications, especially in field emission, surface effects are important. In this paper, we address some properties of the surface of a-C thin films by simulating the deposition of a film using molecular dynamics. Due to the complexity of the chemistry at a surface, we have used a tight-binding approach which explicitly includes a quantum mechanical description of the electrons.

The properties of a-C films show a strong dependence on the deposition energy. A broad peak in many of these properties, such as stress, density and tetrahedral bonding fraction, exists in an energy window from 20 to 500 eV [1]. Despite the numerous experimental studies of a-C films [2–7], there are many unresolved questions surrounding the surface properties, such as the sputtering mechanism and the surface topology. Molecular dynamics simulations provide a valuable insight into such questions, as the atomic positions and trajectories can be followed explicitly.

0953-8984/02/040723+08$30.00

The liquid quench method has been used successfully to model the interior of a-C using a wide range of interatomic potentials [8–14]. However, to model the surface of a thin film on a substrate, it is necessary to simulate the atom-by-atom growth from a sufficiently large number of condensing atoms. While high levels of theory such as the density-functional theory [15] and non-orthogonal tight-binding theory [16] can be applied to the liquid quench, it is not practical to use them in film growths because of the computational cost. To date, film growth simulations have almost exclusively used computationally efficient empirical potentials such as those of Tersoff [14] and Brenner [17] and, most recently, the environment-dependent interatomic potential (EDIP) [18].

Little attention has been given to the surface in the modelling literature, as the focus has been on the study of bonding fractions. Uhlmann *et al* [19] studied the growth processes using a density-functional-based tight-binding potential [16] for energies of 20, 40, 80 eV onto a preprepared a-C surface and found two distinct regimes. Surface processes were found to be dominant for deposition below 30 eV, roughening the surface. Above this, energy subsurface processes were responsible for the film growth, forming 'a low-density, sp^2-rich defective surface layer, the thickness of which scales with the ion range'. The structures present on the surface appear interesting, particularly as they include short sp bonded chains, but no sputtering events were recorded. This study should be regarded as preliminary since fewer than 20 atoms were deposited at each energy, preventing them from observing the evolution of the surface and sputtering events during repeated atomic deposition. Jäger and Albe [20] used a modified Brenner potential to grow sp^3-rich films from more than 1000 carbon-atom impacts on {111} diamond. However, with regard to the surface properties, they confirm, but without detailed analysis, the existence of a 'porous, sp^2-rich surface layer of lower density'. Kaukonen and Nieminen [21] utilized the Tersoff potential to deposit around 300 atoms onto an a-C substrate at four different incident energies. The number of scattered atoms for each of the growths was reported, but their main focus was on determining the growth mechanism at various incident energies. Marks [22] used a generalized form of EDIP that he had developed for carbon [23] to grow films from 500 atoms on a {100} diamond substrate. He found that the top layers of the film deposited with 40 eV atoms were sp and sp^2 bonded with a thickness in good agreement with electron energy-loss measurements at 35 eV.

Recently, Kohary and Kugler [24, 25] undertook the first simulations of film growth using the tight-binding approach, considering only low hyperthermal incident energies below 10 eV. No sputtering events were observed during the fewer than 200 impacts, presumably because of the low incident energies used.

In this work, we use an orthogonal tight-binding approach which is sufficiently efficient to allow the growth of a film from over 500 deposited atoms. This paper presents the first tight-binding, atom-by-atom simulation of carbon thin-film growth at energies relevant to ion-assisted deposition techniques.

2. Method

A pure diamond crystal, with an exposed {001} surface in the experimentally observed 2×1 surface reconstruction was used as the substrate for the simulation. 4×4 unit cells yielded a surface measuring 1.39×1.39 nm and periodic boundary conditions were applied in the x- and y-directions. The substrate depth was chosen to be five unit cells, resulting in a substrate consisting of 640 carbon atoms. Of these, the bottom two unit cells (256 atoms) were coupled to a thermostat at 300 K. Trial collisions demonstrated that incident 100 eV carbon atoms would not penetrate more than two unit cells of a diamond substrate, implying that no crystal deformation would be expected to reach the thermostat layers.

The density-matrix, orthogonal tight-binding method was chosen to describe the atomic interactions because of its combination of good transferability and computational efficiency [26]. A modified form of the tight-binding potential of Xu *et al* [27] was used to model the carbon interactions to make the film growth computationally feasible. The cut-off distances r_m and d_m were reduced from 2.6 to 2.00 Å, whist the match points r_1 and d_1 were reduced to 1.85 Å from 2.45 and 2.57 Å respectively.

In a cathodic arc, typical growth rates of ta-C films (see below) are of the order of 0.1 nm s^{-1}, equivalent to an atomic impact every 0.1 s on the chosen substrate area. However, this timescale is computationally intractable so an artificial process was constructed to replicate the experimental situation.

It has been proposed [19] that there are three different timescales associated with ion deposition processes:

(1) a *collisional* phase including the ion impact and transfer of energy to other atoms in the collision cascade;
(2) a *thermalization* stage characterized by atomic rearrangement and self-annealing of the damaged regions;
(3) a *relaxation* phase during which diffusion is the dominant process.

In our simulation, we included the first two stages but were forced to exclude the third, as diffusion occurs on such long timescales (of the order of milliseconds) that it is computationally inaccessible to tight-binding molecular dynamics simulations. The collisional stage is treated in our simulation using a very short time step of 0.25 fs in order that the equations of motion were integrated correctly for the rapidly moving atoms. Subsequently the time step was increased, firstly to 0.5 fs and then to 1.0 fs as the maximum kinetic energy of the atoms decreased. The total time for this deposition stage was 600 fs. Afterwards, the system was quenched to 0 K over 50 fs to find the local energy minimum before rescaling the velocities to a temperature of 300 K and allowing the structure to equilibrate for 70 fs. This procedure was repeated for each incident atom, thereby simulating the atom-by-atom growth characteristic of cathodic arc deposition.

For this simulation, a cluster is defined to be sputtered when it is no longer bonded to the bulk. These sputtered atoms are removed from the system prior to the quench and re-thermalization, before the next deposition event.

3. Results

3.1. Bulk properties

A total of 535 atoms were deposited onto the substrate, with the grown film having a cross-section shown in figure 1. The amorphous nature of the grown film is shown clearly. The transition from a diamond substrate to a low-coordination surface layer is apparent in figure 2. Further, the low sp^3 content of the bulk region demonstrates that a-C was grown in preference to the highly tetrahedral form of a-C, known as tetrahedral amorphous carbon (ta-C). This result is not in agreement with experiment and represents a limitation of the tight-binding method used by us. There is a prominent spike in the radial distribution function for the bulk region of the film as shown in figure 3. This fictitious spike has arisen from the reduced cut-off distances imposed on the interatomic potential. The spike represents atoms an unphysical concentration of atoms at the maximum interaction range of 2 Å. However, this reduction in the interaction range was necessary to ensure that the simulation was computationally tractable within the density-matrix, orthogonal tight-binding approach. It is important to note that all interatomic

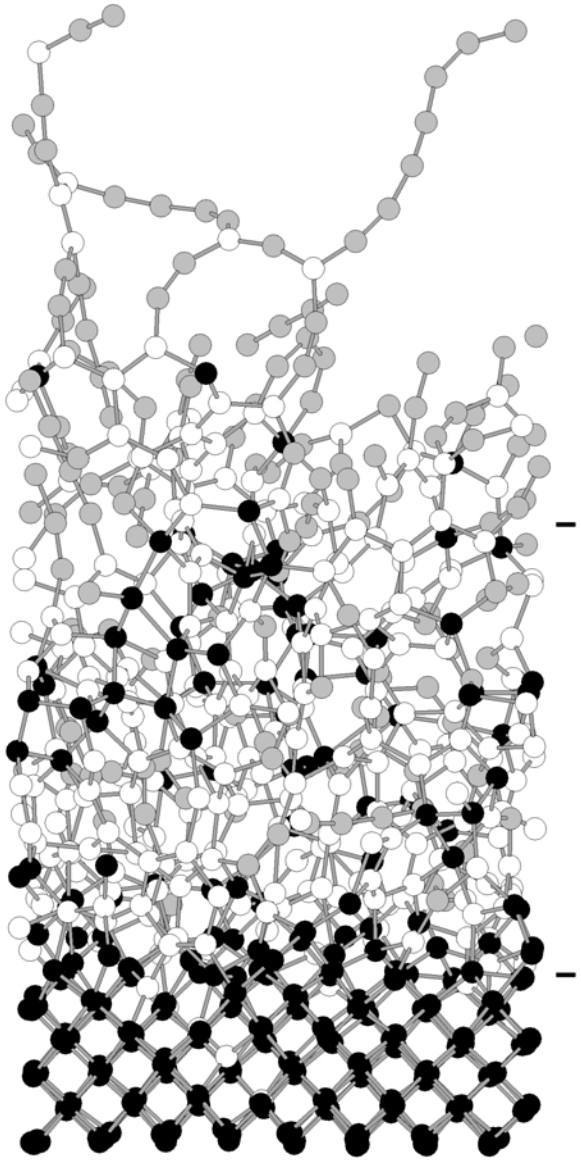

Figure 1. The deposited film. Black atoms have coordination four, white atoms have coordination three, and grey atoms have coordinations two and one. The two tick marks on the right of the figure indicate the substrate/bulk and bulk/surface boundaries.

potentials with a maximum interaction range less than the plane spacing in graphite (3.3 Å) suffer from an important limitation involving the modelling of graphite and therefore graphite-like phases. The short-range interaction precludes any π-orbital repulsion between graphite layers, so it is possible for a sp^2-rich, graphite-like phase to be produced at unphysically high densities, rather than the experimentally observed sp^3-rich, diamond-like phase. This has been noted by Jäger and Albe [20] with reference to the Brenner potential, for which they showed that an interatomic potential with a maximum cut-off range of 2.0 Å 'does not exclude the

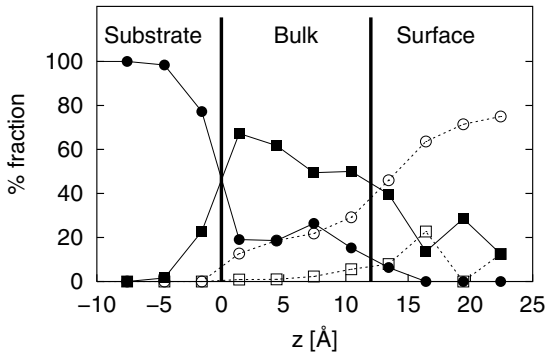

Figure 2. Coordination as a function of depth. Key: 1 = white square, 2 = white circle, 3 = solid square, 4 = solid circle.

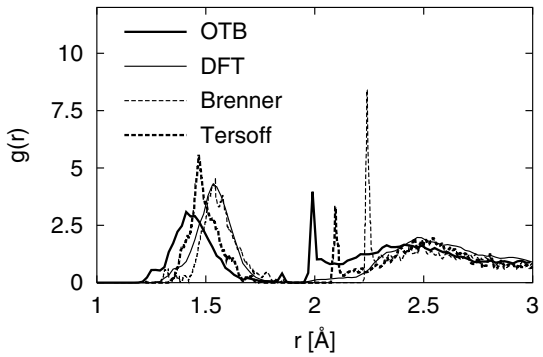

Figure 3. The radial distribution function $g(r)$ for the bulk section of the film as defined by figure 2 compared to the liquid quench results for other interatomic potentials.

occurrence of an artificial *compressed graphite* with a density increase of up to a factor of $3.35/2.0 = 1.675$, exceeding even the density of diamond ($\rho_{\text{diamond}} = 1.56 \times \rho_{\text{graphite}}$)'. This limitation is responsible for the significant underestimation of the sp^3 fraction of the grown film. The short cut-off ranges of these potentials are demonstrated by the spikes shown in figure 3 for the orthogonal tight-binding, Brenner and Tersoff potentials, each of which has a maximum interaction range of less than 3.3 Å. In contrast, no such spike exists in the radial distribution function calculated using density-functional theory for which the interaction range has no such limitation.

3.2. Surface properties

Figure 4 shows the radial distribution function of the surface layer. The absence of any significant spike at 2 Å demonstrates that the reduction in the interaction range in the interatomic potential has not adversely affected the bonding description in the surface layers. The splitting of the first peak in this radial distribution function arises because shorter distances are associated with the surface chains, whilst the porous surface layer contributes the slightly longer distances.

A notable surface feature is the presence of linear chains, which are found throughout the simulation and are stable on this timescale. Indirect evidence for their existence is provided by the sputtering data (figures 5 and 6) since the chains give rise to the sputtered clusters.

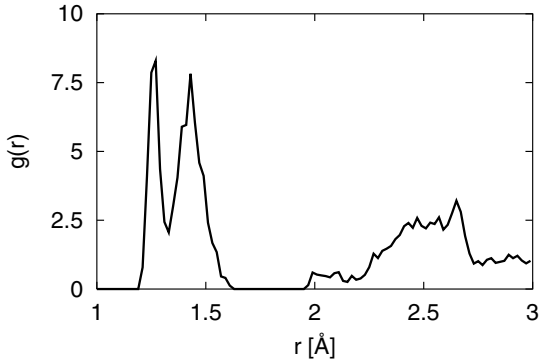

Figure 4. The radial distribution function $g(r)$ for the surface of the film as defined by figure 2.

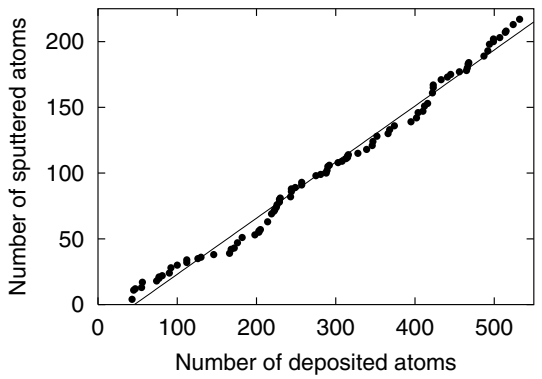

Figure 5. Total number of sputtered atoms as a function of the number of ions deposited. The solid line is a linear fit to the data.

Figure 5 has two important features. The sputter yield is given by the gradient, giving a value of 0.43 which is comparable to the self-sputter yields of 0.47–0.58 at 300 eV and 0.74–0.79 at 600 eV derived from the experimental sticking coefficients of Miyazawa *et al* [28] for a-C films grown on graphite substrates. The non-zero x-intercept of figure 5 shows that sputtering does not occur until after roughly 50 atoms have been deposited, as the surface becomes amorphous.

Figure 6 compares the simulation sputtering result with a normalized and smoothed set of experimental data [29]. The experimental data are fitted using a line of best fit to eliminate the sputter frequency alternation between the odd and even cluster sizes, which is introduced by the method used for measuring the sputter frequency. The negative-ion clusters have a relative distribution which scale with their electron affinity when using mass-spectrometer analysis of negative-ion sputtering products [30]. Therefore the even-numbered chains are measured to be relatively more abundant as they have a high electron affinity owing to their open-shell electronic structures, whereas the odd-numbered chains have a significantly lower electron affinity [31]. The agreement with experiment is very good, though there are obviously significant errors associated with the simulation results owing to the small statistical sample. These errors are larger than the apparent odd–even alternation in the simulation sputter frequencies, requiring a greater number of sputtering events for any conclusion to be drawn regarding whether such an alternation is physically significant.

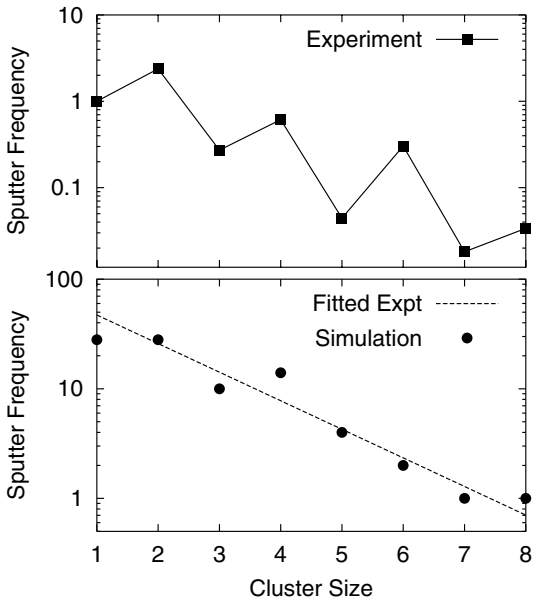

Figure 6. The experimental [29] sputter frequency of clusters (top figure) compared with the simulation results by fitting a line (bottom figure). The experimental results were normalized to the monomer yield.

Two models [30] have been proposed to explain the emission of clusters during sputtering, the model of direct emission and the recombination model of cluster formation. The direct emission model proposes that clusters are formed on the surface, and are ejected intact. The recombination model predicts that only atoms are sputtered, with clusters being formed as a result of the recombination of these atoms which are sputtered independently in the same collision cascade. Whilst there is experimental evidence for both models, Abdullaeva *et al* [30] found that 'clusters mainly leave the sputtered surface as such' during graphite, silicon and aluminium sputtering by alkali metal ions, thereby supporting the direct emission model. Our simulation results also support the direct emission model, as there were only two occurrences of multiple sputtering from a single impact. The resulting two C_2 clusters in one case, and one C and one C_2 cluster in the other, were sputtered in different directions with different velocities, making recombination highly unlikely. Thus our simulation results suggest that the direct emission mechanism completely dominates the recombination mechanism in this system.

Tight-binding [32] and *ab initio* [33] calculations have found that cyclic rings are the more stable state for small carbon clusters ($N \leqslant 10$) with an even number of atoms. Ultraviolet photoelectron spectra of negative-ion clusters [31] show that clusters consisting of 2–9 atoms are linear chains. This result indirectly confirms the presence of chains on the surface during thin-film growth, as it is the sputtering of these chains which produces the linear-only clusters observed experimentally.

4. Conclusions

This paper reports the first tight-binding simulation of carbon thin-film growth at a typical deposition energy of a cathodic arc. The surface properties of this film are in good agreement

with the experimental data, including the variation of the sputter frequency with chain length. Chains were observed to exist on the surface during growth, with these being used to explain why only linear sputtered clusters are observed. A universal shortcoming of short-ranged interatomic potentials has been identified as the cause of the low sp^3 fraction observed in the bulk.

References

[1] McKenzie D R 1996 *Rep. Prog. Phys.* **59** 1611
[2] McKenzie D R, Yin Y, Marks N A, Davis C A, Pailthorpe B A, Amaratunga G A and Veerasamy V S 1994 *Diamond Relat. Mater.* **3** 353
[3] Li F and Lannin J S 1990 *Phys. Rev. Lett.* **65** 1905
[4] Merchant A R, McCulloch D G, McKenzie D R, Yin Y, Hall L and Gerstner E G 1996 *J. Appl. Phys.* **79** 6914
[5] Gilkes K W R, Gaskell P H and Robertson J 1995 *Phys. Rev.* B **51** 12 303
[6] Fallon P J, Veerasamy V S, David C A, Robertson J, Amaratunga G A J, Milne W I and Koskinen J 1993 *Phil. Mag.* B **48** 4777
[7] Schwan J, Ulrich S, Theel T, Roth H, Ehrhardt H, Becker P and Silva S R P 1997 *J. Appl. Phys.* **82** 6024
[8] Galli G, Martin R, Car R and Parrinello M 1989 *Phys. Rev. Lett.* **62** 555
[9] Marks N A, McKenzie D R, Pailthorpe B A, Bernasconi M and Parrinello M 1996 *Phys. Rev. Lett.* **76** 768
Marks N A, McKenzie D R, Pailthorpe B A, Bernasconi M and Parrinello M 1996 *Phys. Rev.* B **54** 9703
[10] McCulloch D G, McKenzie D R and Goringe C M 2000 *Phys. Rev.* B **61** 2349
[11] Drabold D A, Fedders P A and Stumm P 1994 *Phys. Rev.* B **49** 16 415
[12] Stephan U, Frauenheim Th, Blaudeck P and Jungnickel G 1994 *Phys. Rev.* B **50** 1489
[13] Wang C Z and Ho K M 1994 *Phys. Rev.* B **50** 12 429
[14] Tersoff J 1988 *Phys. Rev. Lett.* **61** 2879
[15] Car R and Parrinello M 1985 *Phys. Rev. Lett.* **55** 2471
[16] Porezag D, Frauenheim Th, Koehler Th, Seifert G and Kaschner R 1995 *Phys. Rev.* B **51** 12 947
[17] Brenner D W 1990 *Phys. Rev. Lett.* **42** 9458
[18] Justo J F, Bazant M Z, Kaxiras E, Bulatov V V and Yip S 1998 *Phys. Rev.* B **58** 2539
[19] Uhlmann S, Frauenheim Th and Lifshitz Y 1998 *Phys. Rev. Lett.* **81** 641
[20] Jäger H U and Albe K 2000 *J. Appl. Phys.* **88** 1129
[21] Kaukonen M and Nieminen R M 2000 *Phys. Rev.* B **61** 2806
[22] Marks N A 2002 *J. Phys.: Condens. Matter* submitted
[23] Marks N A 2000 *Phys. Rev.* B **63** 035401
[24] Kohary K and Kugler S 2000 *J. Non-Cryst. Solids* **266-269** 746
[25] Kohary K and Kugler S 2001 *Phys. Rev.* B **63** 193404
[26] Goringe C M, Bowler D R and Hernández E 1997 *Rep. Prog. Phys.* **60** 1447
[27] Xu C H, Wang C Z, Chan C T and Ho K M 1992 *J. Phys.: Condens. Matter* **4** 6047
[28] Miyazawa T, Misawa S, Yoshida S and Gonda S 1984 *J. Appl. Phys.* **55** 188
[29] Pargellis A N 1990 *J. Chem. Phys.* **93** 2099
[30] Abdullaeva M K, Atabaev B G and Dzabbarganov R 1991 *Nucl. Instrum. Methods* B **62** 43
[31] Yang S, Taylor K J, Craycraft M J, Conceicao J, Pettiette C L, Cheshnovsky O and Smalley R E 1988 *Chem. Phys. Lett.* **144** 431
[32] Menon M, Subbaswamy K R and Sawtarie M 1993 *Phys. Rev.* B **48** 8398
[33] Raghavachari K and Binkley J S 1987 *J. Chem. Phys.* **87** 2191